JOURNAL OF
EMERGING INVESTIGATORS

Article

In silico design of an epitope-based vaccine for Rocio virus using phage display & *E. coli* expression system

Taarun Ganesh[1], Jarin Taslem Mourosi[2]

[1] Thomas Jefferson High School for Science and Technology, Alexandria, Virginia

[2] Department of Biology, Catholic University of America, Washington, D.C.

SUMMARY

The Rocio virus, a member of the Flaviviridae family transmitted by *Culex* mosquitoes, causes headaches, fever, confusion, and fatal neurological symptoms. Currently, there is no approved vaccine available for the virus. Traditional Flaviviridae vaccine platforms rely heavily on live attenuated or inactivated viruses, which have significant limitations regarding safety. Here, we hypothesized that computational tools could be used to develop an epitope-based vaccine integrating M13 bacteriophage by generating epitopes that elicit a strong immune response against the Rocio virus. Using bioinformatics tools, we analyzed the proteome of the Rocio virus and selected 30 key B and T cell epitopes based on their antigenicity, allergenicity, and toxicity scores. We demonstrated both a phage-based epitope display and fusion epitope production using a bacterial expression system. In the phage-based delivery mechanism, a minor coat protein (pIII) of M13 bacteriophage was fused with the epitopes. Conversely, in the *E. coli* expression system, we designed the vaccine candidate by joining predicted epitopes with linkers to create a final antigenic product. Through molecular docking, we identified that the vaccine candidate binds effectively with antigen receptors and induces a robust immune response with an *in silico* immune simulation. Overall, this computational approach allows for the rapid generation of epitopes and demonstrates a novel framework combining bacteriophage display and bacterial expression. Nevertheless, further *in vitro* and *in vivo* experiments are essential to evaluate the candidate's safety, efficacy, and ability to neutralize the virus.

INTRODUCTION

Rocio virus (ROCV) is a single-stranded RNA virus that belongs to the *Flaviviridae* family and is transmitted through the bite of *Culex* mosquitoes (1). The ROCV genome is approximately 11 kilobases long (1). This ROCV genome encodes three structural proteins: pre-membrane (prM), envelope (E), and capsid (C) proteins, which are involved with the structure and assembly of the virus and enable it to enter host cells (1). ROCV also has seven nonstructural proteins (NS1, NS2A, NS2B, NS3, NS4A, NS4B, and NS5), which are involved in the replication of viral RNA (2). ROCV infection causes a variety of symptoms: encephalitis, fever, severe headache, vomiting, blindness, and conjunctivitis (3). ROCV initially emerged in Brazil in 1975 during an encephalitis outbreak, with a total of 465 infections and a 13% case fatality rate. Among the 465 cases, approximately 20% of patients developed neuropsychiatric conditions, including dysarthria and motor impairment (4). Researchers initially developed a formalin-inactivated ROCV vaccine and administered 3 doses over the course of 1 month, followed by a booster dose 15 months later (3). However, that vaccine was discontinued due to a low seroconversion rate of 22%, which indicated that the vaccine did not stimulate a sufficient antibody response (5).

Following the 1975 outbreak, there is a lack of documentation describing how ROCV continued to circulate in the environment. Serological evidence suggests that ROCV was carried asymptomatically through migratory bird species, along with *Aedes* and *Psorophora* mosquitoes, possibly accounting for ROCV's disappearance after the initial outbreak (6). In 2011, 9 ROCV strains were recovered using central nervous system tissue from a total of 17 deceased patients during a dengue virus (DENV) outbreak in Goiás, a central Brazilian state (3). Using serum samples from patients of all ages and sexes with suspected dengue fever, Saivish et al. identified the ROCV NS5 gene, and confirmed, through phylogenetic analysis, that it was a 100% match to an isolated ROCV strain from the original 1975 encephalitis outbreak (3). These findings imply that ROCV may have continued to circulate undetected throughout South America, despite the absence of reported cases between 1975 and 2011. As such, there is a high probability that ROCV is still circulating throughout South America, highlighting the need for further research to prevent reemergence. Currently, no licensed vaccine is available for ROCV.

In this study, we used bioinformatic tools to develop a multi-epitope-based vaccine candidate for ROCV. Epitopes are short peptide fragments derived from viral proteins that are recognized by the immune system, allowing antibodies and T cell receptors to elicit an immune response in response to the pathogen (7). Three different categories of epitopes were predicted from the structural and non-structural proteins of ROCV: epitopes recognized by B cells, CD8+ T cells, and CD4+ T cells. In this context, B cells produce antibodies, which bind to specific antigens to fight off pathogens. CD8+ T cells (often referred to as cytotoxic T cells) primarily provide protection by directly killing virally-infected cells, while CD4+ T cells (often referred to as helper T cells) can signal other immune cells for activation and also produce cytokines that aid B cells in the synthesis of antibodies (8). Peptides that are presented by major histocompatibility complex (MHC) Class I molecules are recognized by CD8+ T cells, while those presented by MHC Class II molecules are recognized by

https://doi.org/10.59720/24-279

CD4+ T cells (8). It is vital that epitopes capable of activating B cells, CD8+ T cells, and CD4+ T cells are included in the vaccine candidate to ensure that the candidate provides a strengthened (virus-specific) immune response (8). The predicted epitopes were screened for favorable biophysical characteristics for incorporation into the final vaccine candidate, including antigenicity, allergenicity, and toxicity. Antigenicity is defined as the characteristic of an antigen to be recognized by the immune system and produce an immune response, while allergenicity is the ability of an antigen to provoke an abnormal immune response, causing the unfavored effect of tissue damage. Likewise, toxicity refers to the potential of a peptide to cause damage to the cell.

Epitope-based vaccines provide a targeted immune response against an immunodominant epitope and are safer than live attenuated vaccines, which use the entire virus for vaccine development (7, 9). Rather than using whole pathogens or large proteins, epitope-based vaccines use specific protein fragments (epitopes) from a pathogen to stimulate an immune response, enhancing specificity and safety (9). An *in silico* vaccine design refers to the process of designing and selecting vaccine epitopes using computational methods, and epitope-based vaccines have been initially developed by *in silico* methods to improve efficiency. Successful implementations of *in silico* vaccines have been developed for cancer and viral infections, such as similar flaviviruses like the dengue and Zika virus (10, 11). For instance, epitope-based vaccines for the Zika virus developed using an immunoinformatic approach have demonstrated promising outcomes and usefulness in subsequent *in vitro* and *in vivo* studies, with processes including molecular docking and immune simulation supporting their potential efficacy (12). These vaccines have exhibited stability and have progressed to phase I and II clinical trials, suggesting that an effective vaccine could be generated for ROCV through similar methods (13, 14).

With the rapid development of computational biology tools, epitopes can be predicted, and multiple rounds of screening can be performed based on different parameters to determine a vaccine candidate (15). The delivery mechanism of a vaccine is a critical part of eliciting a potent immune response. Phage display represents a versatile platform for antigen presentation and was employed in this study to enable surface display of peptide epitopes with high immunogenicity. In phage display systems, the DNA encoding foreign antigens are fused to genes encoding phage surface proteins, resulting in the expression of fusion proteins displayed on the phage surface by production in bacteria or direct incorporation in the phage genome (16, 17). Here, we used an M13-based display, where the surface protein pIII (a minor coat protein) was utilized to incorporate the epitopes. M13 phage display is highly immunogenic and is also capable of displaying larger peptides and proteins without hampering its replication (18, 19). Additionally, M13 has a non-lytic life cycle, which allows continuous phage production without killing their host bacteria, resulting in higher phage yield (20). Vaccines made with the phage-based system are safer than live attenuated vaccines, inexpensive, adjuvant-free (DNA vaccines require an adjuvant), and delivered intranasally/orally. These vaccines are also more likely to be globally accessible, as they can be rapidly produced and are stable at various pHs and temperatures for ease of storage (16, 21). However, many phage-based vaccines are currently only in early clinical trials or a preclinical stage (22).

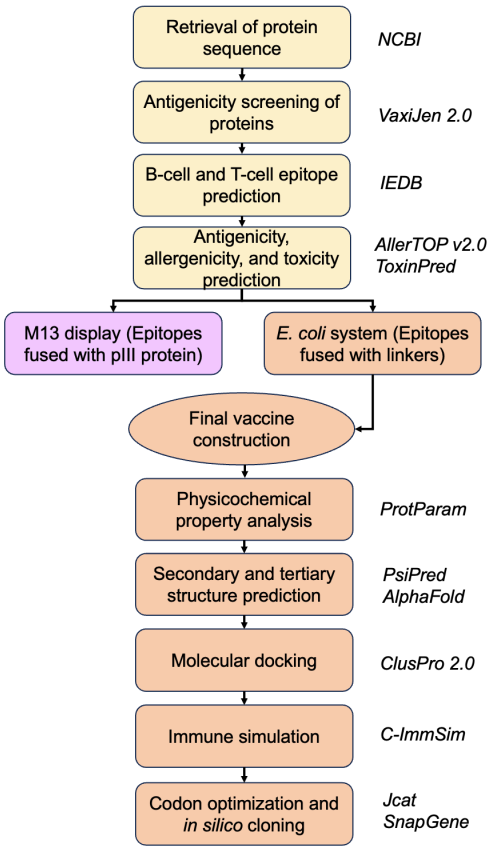

Figure 1: Methodical procedures utilized to identify and formulate a Rocio virus vaccine. This figure shows the overall workflow of the study. After we retrieved the Rocio virus (ROCV) polyprotein sequence from NCBI and screened the ROCV proteins using the VaxiJen 2.0 server, we predicted B-cell and T-cell epitopes using the Immune Epitope Database (IEDB) server (27, 28). We assessed the antigenicity using VaxiJen, predicted allergenicity using AllerTOP v2.0 and toxicity using ToxinPred servers (57, 59, 60). The study displayed a vaccine candidate using both the M13 bacteriophage system and the *Escherichia coli* system. We analyzed the amino acid sequence of the final vaccine candidate using ProtParam (49). We predicted the vaccine candidates secondary structure using PsiPred, and tertiary structure (3-D structure) using AlphaFold (31). We docked the vaccine candidate against antigen receptors BCR, CD4+ T cell, and CD8+ T cell using ClusPro 2.0 (34). We predicted the immune simulation using the C-ImmSim server (35). Finally, we performed codon optimization using JCat and conducted *in silico* cloning using SnapGene software (36, 80).

Additionally, we also used an *E. coli* bacterial expression system to express the multi-epitope fusion protein, providing a different approach of epitope delivery. The vaccine production in *E. coli* is scalable and low-cost with simple culture conditions; however, *E. coli* cannot perform post-translational modifications and falls short in protein folding and endotoxin removal (23). The lack of proper protein folding in an *E. coli* expression can lead to altered or nonfunctional proteins,

https://doi.org/10.59720/24-279

which could compromise the vaccine's stability and efficacy. Likewise, bacteria-derived endotoxins can create an adverse immune response in the human body and subsequently hinder the quality of vaccine production (24). In contrast, mammalian expression systems can perform complex post-translational modifications such as glycosylation and phosphorylation, which help ensure proper protein folding and stability (25). Nevertheless, these mammalian systems are slower, more expensive to maintain, and often yield lower protein amounts as compared with bacterial systems. Thus, bacterial systems still remain promising for their cost-effectiveness and scalability for protein production (25).

Thus, this study designed a potential epitope-based vaccine to combat future outbreaks of ROCV. Leveraging advanced computational biology tools, we identified potential antigenic, non-allergenic, and non-toxic epitopes from the ROCV genome. We hypothesized that conducting a computational study using bioinformatics methods could create a ROCV vaccine candidate that would produce a potent immune response. With a high antigenic score predicted from our modeling, our vaccine construct shows potential for effective immunization against ROCV, representing an important step toward developing a licensed vaccine for this pathogen, which is associated with severe neurological complications in infected patients. This study serves as a promising initial step in the development of a vaccine for ROCV, with additional experiments needed to evaluate these results and advance towards pre-clinical developments and clinical trials.

RESULTS

Due to the lack of a licensed vaccine for ROCV, there is a need for an alternative approach to rapidly design a safe and effective vaccine candidate. In this study, we hypothesized that a bioinformatics-driven approach could be used to identify antigenic, non-allergenic, and non-toxic epitopes to construct a multi-epitope vaccine candidate that can elicit a strong immune response.

Epitope-based vaccine design workflow

In this study, we utilized various bioinformatics tools to aid us in designing an epitope-based vaccine for ROCV. We first retrieved the ROCV polyprotein sequence and tested for antigenic proteins to use in epitope prediction. Next, from these antigenic proteins, we predicted B-cell and T-cell epitopes, which we later extensively screened for antigenicity, allergenicity, and toxicity. Then, we incorporated linker sequences between each epitope to construct our final vaccine candidate. With the vaccine candidate, we conducted a protein-protein docking analysis with three antigen receptors

Type	Sequence	Antigenicity Score	Toxicity (SVM) Score	IFN Score
CD8+ T Cell	VVEEHKGIY	0.4231	-1.31	—
	TTSILFVSY	0.9915	-1.21	—
	MTSGVLGSY	0.9458	-1.55	—
	TMNAADNLY	0.4011	-0.06	—
	ITSQASALF	0.4325	-1.29	—
	ALFGLNSGY	0.9769	-0.71	—
CD4+ T Cell	RNPGYAIVAVAAAWM	0.7317	-0.95	0.3478
	RQTVVALAAQEGALH	0.7737	-0.91	0.0809
	TRQTVVALAAQEGAL	0.8285	-0.71	0.2780
	LIAVFNIQPAALVST	1.1522	-1.79	0.4792
	ALAWMILKAVSIGTV	1.2327	-1.64	0.6083
	AMALAWMILKAVSIG	1.3382	-1.77	0.4071
	FHTMWHVTQGAALRN	0.5452	-0.93	0.1801
	TEEVQLIAAEPGKPV	0.4232	-1.31	1.0000
	HRRDLRLMANAICSA	0.5954	-0.63	0.0916
B Cell	TYECPRLEPGMDPED	0.9293	-0.90	—
	SHGESQLENRGTPWLDTAKTTK	0.7443	-1.27	—
	PTSVAAHGNYTTQLGAKHA	0.8056	-1.11	—
	FHDLDLPWTGPATDVWKNRE	0.7319	-0.55	—
	PETKECPTERRAWN	0.4113	-1.50	—
	TWEEEAEITGTSPR	0.8071	-0.96	—
	DLPAPKQMGRSDM	0.5832	-0.61	—
	AYVSAISQGERQEEEAPEAF	0.6999	-1.60	—
	INYTDRRWCFDGPHNNTILEDN	0.8047	-0.71	—
	EKGGRAHRAALE	0.7870	-0.51	—
	EAPKVKRGGIA	0.5821	-1.03	—
	GKREKKLGEFGKAKG	1.3499	-0.37	—
	GYTKGGPGHEEPMLMQS	0.5022	-1.38	—
	FEEQNQWASAREAVEDPGFWNL VDKERQAHLEG	0.5033	-1.12	—
	KDHRKGPRYEEDVDLGSGTRSV ARRSPFMDTRKIHH	0.9320	-0.47	—

Table 1: Final epitopes selected for the ROCV vaccine candidate. This table lists 30 epitopes from ROCV that were screened based on their predicted ability to be recognized by CD8+ T cells, CD4+ T cells, and B cells. The antigenicity score and the toxicity score, with respective thresholds of 0.4 and 0, are listed for all epitopes, while the IFN score is only applicable to the CD4+ T cell epitopes.

https://doi.org/10.59720/24-279

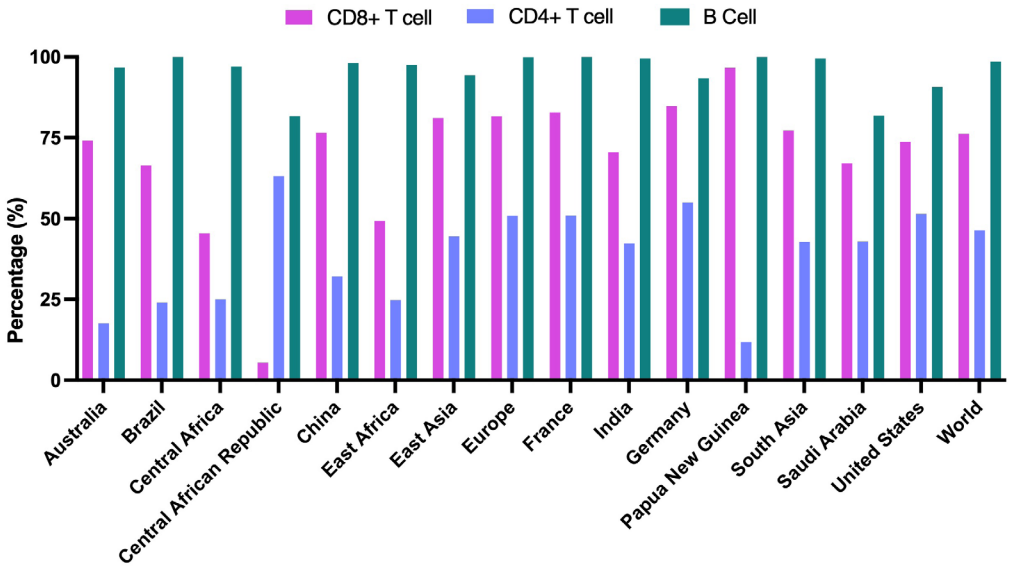

Figure 2: Population coverage analysis of the selected epitopes and their chosen MHC alleles. The bar graph shows the percentage (%) of individuals in selected countries that were predicted to respond to a particular set of epitopes based on human leukocyte antigen (HLA) genotypic frequencies. Each bar represents the percentage of individuals within a given country predicted to have activation of a specific immune cell type (CD8+ T cells, CD4+ T cells, or B cells) by the selected epitopes. Percentages were calculated through IEDB.

– a cytotoxic T cell receptor, a helper T cell receptor, and a B cell receptor (BCR) – and performed an immune simulation to assess the efficacy of the candidate vaccine. Following codon optimization of the candidate, we performed *in silico* restriction cloning for insertion into a plasmid **(Figure 1)**.

Antigenicity determination of the proteins and epitope screening

Initially, to predict potential antigenic epitopes from the ROCV proteome, we retrieved the FASTA format of the ROCV polyprotein sequence and used the online antigenicity prediction tool VaxiJen v2.0 to assess antigenicity for each structural and non-structural protein (26, 27). Only the capsid protein was non-antigenic from the server prediction, while the remaining proteins were antigenic (data not shown). We generated possible epitopes using the Immune Epitope Database (IEDB) server and conducted extensive screening of antigenicity, allergenicity, toxicity, human proteome non-homology, and cytokine-inducing potential, focusing on interferon-gamma (IFN-γ) and interleukin-10 (IL-10) responses (28). By predicting human proteome non-homology, we can minimize the risk of cross-reactivity with human proteins, which would otherwise lead to unintended autoimmune responses. IFN-γ is a cytokine that drives MHC Class I expression and activates helper T cells; predicting the IFN-γ response helps ensure the vaccine induces a protective immune response to eradicate the virus. Similarly, IL-10 functions as an anti-inflammatory cytokine that enhances B cell differentiation and proliferation, contributing to long-term protection against the virus (29). With respective non-allergen and non-toxin labels provided by the AllerTOP v2.0 and ToxinPred server, this screening identified the most promising 6 CD8+ T cell, 9 CD4+ T cell, and 15 B cell epitopes, based on antigenicity, toxicity, and IFN-γ-inducing potential, among other characteristics **(Table 1).**

Population coverage analysis of selected peptides

Next, to measure the effectiveness of our vaccine peptides in different populations, we used the IEDB server to calculate the population coverage for each epitope with specific MHC-restricted alleles (28). Using an epitope set based on human leukocyte antigen (HLA) genotypic frequencies, which represent the human-specific form of MHC molecules, the IEDB server provides a percentage of individuals in a certain population that respond to the given sequence. The analysis showed that the CD8+ T cell epitopes covered 76.26% of the world population, while the CD4+ T cell epitopes encompassed 46.43% of the world population; overall, the population coverage for the CD8+ T cell epitopes was higher than that of the CD4+ T cell epitopes. Additionally, the B cell epitopes were predicted to cover 98.58% of the world population, likely due to the number and sheer length of the epitopes incorporated into the final ROCV vaccine candidate. Brazil's population had the highest coverage for the B cell epitopes (99.98%), followed by Papua New Guinea (99.95%) and South Asia (99.52%) **(Figure 2)**.

These results show the developing potential for the ROCV vaccine candidate towards broad immunogenicity, especially due to the high coverage of the B cell and cytotoxic T cell epitopes. This suggests that epitopes with broad HLA binding profiles are essential for ensuring coverage in various populations, and that further refinement of the CD4+ T cell epitope inclusion could enhance the vaccine's overall effectiveness (30).

Biophysical properties of final vaccine construct using *E. coli* expression

Using the selected CD8+ T cell, CD4+ T cell, and B cell epitopes, we assembled the final multi-epitope vaccine construct **(Figure 3a)**. The VaxiJen v2.0 server score for the vaccine construct was 0.6597, which was predicted to be antigenic above the set threshold of 0.4 **(Figure 3b)** (27).

https://doi.org/10.59720/24-279

(a)

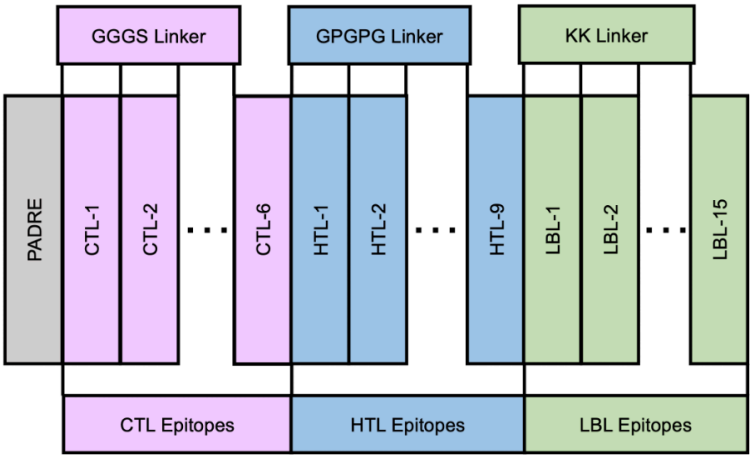

(b)

Properties of Final Vaccine Candidate	
Antigenicity Score	0.6597
Molecular Weight (kDa)	62.059
Instability Index	36.75
Aliphatic Index	59.93
Intrinsic Solubility Score	2.021
Theoretical pI	9.62
Half-life in mammalian reticulocyte (hours)	4.4
Half-life in *E. coli* (hours)	>10
Half-life in yeast (hours)	>20

Figure 3: Schematic depiction and characteristics of the final proposed ROCV vaccine candidate. (a) The immunogenicity-enhancing PADRE sequence (AKFVAAWTLKAAA) was added at the beginning of the vaccine candidate sequence. The cytotoxic T lymphocyte (CTL) epitopes were connected with the GGGS linker, the helper T lymphocyte (HTL) epitopes were linked via the GPGPG linker, and the linear B cell (LBL) epitopes were fused with the KK linker, formulating a final vaccine candidate with 584 amino acids. (b) Biophysical properties of the final vaccine candidate generated by various bioinformatics servers.

Additionally, the molecular weight of the vaccine construct was predicted to be 62.059 kDa, making it favorable for expression in *E. coli* with a weight below 110 kDa. With an instability index (II) of 36.75 computed using the Expasy ProtParam server, the candidate is classified as stable, under the threshold of 40, and with a high aliphatic index of 59.93, the protein demonstrates stability over a wide variety of temperatures. The overall CamSol intrinsic solubility score of the vaccine candidate was predicted to be 2.021, which corresponds with a high solubility, as scores above 1 are denoted high solubility while scores below -1 are denoted with low solubility. The vaccine candidate was also computed to demonstrate basic properties with a predicted theoretical pI score of 9.62, above the neutral pI 7. The vaccine's half-life was predicted to be approximately 4.4 hours in mammalian reticulocytes, with more than 10 hours predicted in *E. coli* and longer than 20 hours predicted in yeast.

Molecular docking with antigen receptors

Next, to perform molecular docking, we predicted the vaccine candidate's 3D structure using the AlphaFold server (31) **(Figure 4a)**. Molecular docking between vaccine structure and antigen receptors is useful in predicting the binding affinity and verifying whether the vaccine candidate can elicit immune responses. We focused on the antigen receptors BCR, CD4+, and CD8+, which are known to recognize peptides and proteins. BCR is a major antigen receptor expressed by B cells that facilitates the processing of antigens, acting as a sensor to antigen binding. Additionally, BCR facilitates antigen processing and internalization in B cells, enabling peptide presentation on MHC Class II molecules, resulting in the activation of helper T cells (32). On the other hand, computational docking simulations with T cell receptors from CD4+ T cells and CD8+ T cells have been successful in modeling interactions with other mosquito-transmitted viruses, with top clusters exhibiting favorable binding scores and stable binding conformations (33). Based on this prior success, a CD4+ T cell receptor and CD8+ T cell receptor were selected for docking with the vaccine candidate. The three antigen receptors were docked with their respective portion of the vaccine candidate using the ClusPro 2.0 server, which generated a thousand different conformations with high binding affinities and ranked the top thirty models by cluster size (the number of docked structures) (34). Since cluster size is directly related to the binding affinity between the candidate and the receptor, we selected the highly clustered models for the BCR, CD4+ T cell receptor, and CD8+ T cell receptor. Each model demonstrated cluster sizes of 49, 43, and 161, with lowest energy levels of -1149.2, -1066.0, and -1052.4, respectively **(Figure 4b–e)**. These low energy levels indicate a higher binding affinity with the target protein.

Immune simulation

To predict the immunogenicity of the vaccine candidate, we utilized the C-ImmSim server to conduct an immune simulation study (35). The prediction demonstrated an increase in antibody level (IgM and IgG) following vaccine administration **(Figure 5a)**. Moreover, the vaccine induced the production of CD4+ T cells and CD8+ T cells, a crucial component of cell-mediated immune response **(Figure 5b, 5c)**. However, cytotoxic memory T cells were not detected in the simulation (data not shown). The server also predicted that the ROCV vaccine would stimulate many major cytokines, such as IFN-γ, IL-2, and IL-10, that would notify the immune system that a foreign particle was detected **(Figure 5d)**. In summary, the immune simulation demonstrated that the vaccine candidate could produce a vigorous immunological response.

Codon optimization and *in silico* cloning

Following the immune simulation, we performed codon optimization on the vaccine DNA sequence to increase protein production in *E. coli* using the JCat server (36). The Codon Adaptation Index (CAI) value was 1.0, and the

https://doi.org/10.59720/24-279

(a)

Model #	B Cell Receptor		CD4+ T Cell Receptor		CD8+ T Cell Receptor	
	Cluster Size	Lowest Energy Level	Cluster Size	Lowest Energy Level	Cluster Size	Lowest Energy Level
1	49	-1149.2	43	-1066.0	161	-1052.4
2	32	-1127.1	34	-922.8	148	-967.9
3	29	-1146.0	34	-977.3	98	-923.8
4	28	-1204.9	31	-902.9	67	-916.5
5	25	-1139.9	29	-875.0	63	-886.6

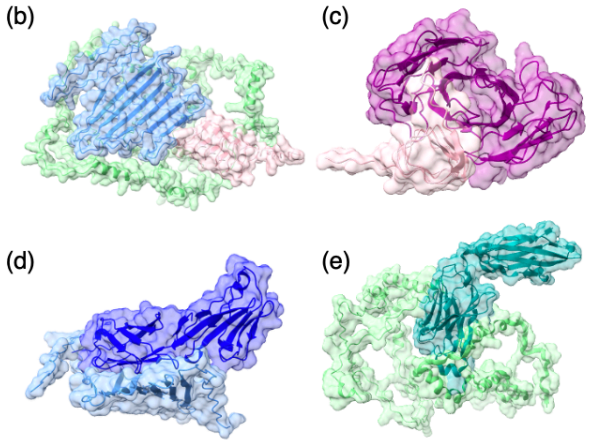

Figure 4: 3D structure prediction and molecular docking of the vaccine candidate. (a) Cluster sizes and lowest energy levels of the five highest ranking models produced by ClusPro 2.0 (34) (b) 3D structure of ROCV vaccine candidate predicted by AlphaFold (contains nine alpha helices). Here, amino acids 1–91 are colored in light pink (CD8+ T cell epitopes), amino acids 92–271 are colored in light blue (CD4+ T cell epitopes), and amino acids 271–584 are colored in light green (B cell epitopes). (c) Docking of CD8+ T cell receptor (magenta) with the CD8+ T cell epitopes of the ROCV vaccine candidate (light pink). (d) Docking of CD4+ T cell receptor (navy blue) with the CD4+ T cell epitopes of the ROCV vaccine candidate (light blue). (e) Docking of BCR receptor (teal) with the BCR epitopes of the ROCV vaccine candidate (light green).

guanine-cytosine (GC) content was 53.03%. This optimized vaccine DNA sequence was incorporated into the pET-28b vector plasmid using the *XhoI* and *NheI* restriction enzyme sites **(Figure 6)**. Subsequently, the RNAfold server was used to generate the mRNA secondary structure of the vaccine, resulting in a minimum free energy score of -612.70 kcal/mol (**Figure 6**). This suggests the vaccine's mRNA has a structure that is both thermodynamically-favored and stable, which would likely maintain mRNA translation efficiency and vaccine efficacy as reinforced by the Gibbs equation (37).

DISCUSSION

In this study, we aimed to create a vaccine candidate using bioinformatics approaches to design a safe and effective multi-epitope vaccine candidate against ROCV, which currently has no licensed vaccine. We hypothesized that a computational immunoinformatics approach could be used to identify antigenic, non-allergenic, and non-toxic epitopes capable of producing a robust immune response. To address this, we analyzed the ROCV proteome using computational tools, selected 30 candidate B and T cell epitopes, and incorporated them into our vaccine construct using both a bacteriophage and bacterial expression system. Our findings indicate that the proposed final vaccine candidate demonstrates predicted high antigenicity, other favorable biophysical properties, strong binding affinity to human antigen receptors, and a capability to induce a robust immune response against ROCV.

Building on this approach, our study screened all of the predicted antigenic ROCV proteins (Pr, M, E, NS1, NS2A, NS2B, NS3, NS4A, NS4B, NS5) to identify optimal epitopes, in contrast to an *in silico* drug repurposing study conducted by Sagini et al., which focused solely on the NS1 protein (2). High antigenicity, low toxicity, and low allergenicity ensure the prevention of disease and safe vaccine administration. Subsequently, the predicted epitopes that could produce an effective immune response were incorporated into our final vaccine construct, which included 6 CD8+ T cell, 9 CD4+ T cell, and 15 B cell epitopes.

Here, we used two different models to display vaccine antigen. In the first model, the pIII protein of M13 bacteriophage fused with the epitopes. The N-terminal domain of pIII is attached with a flexible linker GGGS to incorporate large epitopes. The M13 phage display is known uniquely through its ability to use genetic modification to display proteins on the targeted coat proteins (38). While pVIII has a greater copy number, it only efficiently displays peptides up to eight amino acids in length, so we selected pIII over pVIII (39).

When constructing the *in silico* vaccine for *E. coli* display, we incorporated the PADRE sequence and three linkers (GGGS, GPGPG, and KK). The universal PADRE sequence (AKFVAAWTLKAAA) has been shown to induce a long-lasting antigenic response and is also specifically designed to elicit an enhanced immune response in humans, thereby enhancing the overall immunogenicity of our vaccine (40, 41). To combine the cytotoxic T cell epitopes, the GGGS linker was shown to be a more efficient linker than the AAY linker; it has been reported that the GGGS linker induces a stronger T cell immunological response than the AAY linker for an epitope-based vaccine designed for HIV-1 (42). These glycine-rich linkers strengthened epitopes' flexibilities while preventing undesired interactions (43). The GPGPG linker specializes in stimulating effective responses from the helper T cell epitopes, which is an essential function of a multi-epitope vaccine (44). Lastly, the KK linker, linking the B cell epitopes, reduces junctional immunogenicity (45). The KK linker is also the target for the lysosomal protease Cathepsin B, which helps during antigen presentation (45).

Using the ClusPro molecular docking server to generate a model, we found that the BCR, CD4+ T cell receptor, and CD8+ T cell receptor exhibited a very high binding affinity with the target protein at a low energy level. This interaction highlights the increased affinity between the vaccine candidate and the antigen receptor, promoting strong antiviral immune responses through ligand recognition (46, 47). The molecular weight of our vaccine construct was 62.059 kDa, making it favorable for *E. coli* expression, since proteins less than 110 kDa have a higher chance of being soluble (48). The vaccine candidate's instability index was also calculated to be 36.75, falling under the maximum of 40, demonstrating its

https://doi.org/10.59720/24-279

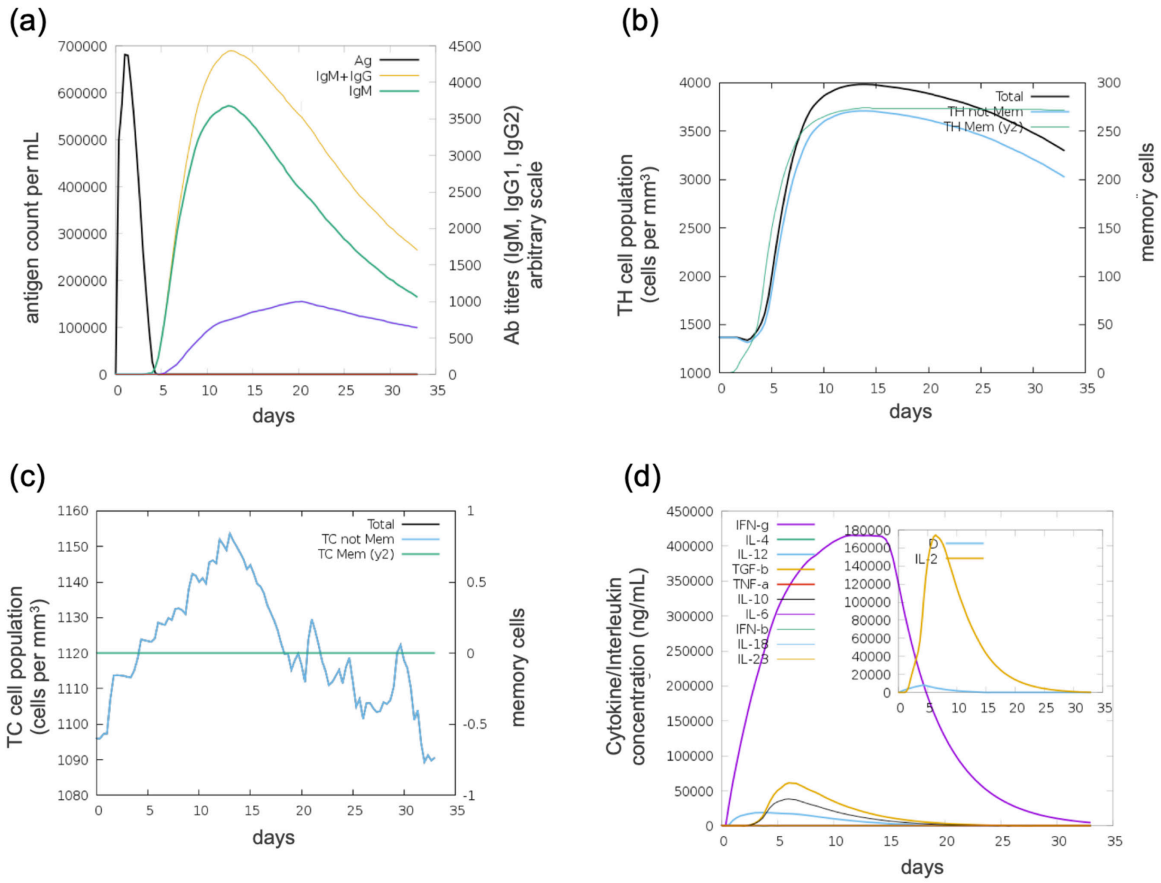

Figure 5: Immune simulation analysis by the C-ImmSim server. (a) Prediction of antibody (Ab) titers, where an increase in various subtypes of antibodies (IgG, IgM) is demonstrated. (b) Predicted count of CD4+ T helper cells by vaccine antigen. (c) Predicted count of CD8+ T cells following vaccination with the vaccine candidate, with an increased level of CD8+ cytotoxic T cells predicted. (d) Prediction of cytokine production, where major cytokines (IFN-γ, IL-10, etc.) are stimulated by the vaccine candidate.

stability under standard conditions (49). The aliphatic index was 59.93, indicating moderate stability across a range of temperatures (50). The proposed vaccine is basic and strongly hydrophilic, with a basic theoretical pI of 9.62 and a negative grand average of hydropathy (GRAVY) value of -0.656 (51, 52). The GRAVY value reflects an average hydropathy value for the entire protein sequence; positive values indicate hydrophobicity, while negative values, as seen here, indicate hydrophilicity. Additionally, the vaccine candidate's intrinsic solubility score is 2.021, above the threshold of 1, which is solubility-promoting.

Utilizing online immune stimulation software, we predicted the immune response of our vaccine candidate. Any ideal vaccine should induce strong antibody-mediated (humoral) immunity and a cellular immune response. After three rounds of injection stimulation, active B cells were present. When B cells are activated, they produce either a memory B cell or a plasma cell, and the plasma cell later produces antibodies, which will protect against ROCV (53). Also, there was an increase in different types of antibody levels, including IgG1 and IgM. Immunoglobulin G (IgG), which is mainly found in bodily fluids, directly neutralizes the virus by activating the complement system, where a cascade of immune proteins either kills the virus directly or facilitates destruction of the pathogen by a phagocytic cell (54). IgG1 specifically is mainly responsible for thymus-mediated immune response and can also bind the Fc receptor of phagocytic cells and activate the complement system (54). IgM, the first antibody produced after virus infection, provides the first line of defense against virus infection (54). There was an upregulation of cytokines such as IFN-γ, IL-2, and IL-10. IFN-γ activates the macrophage and also stimulates the T cell response; IL-2 helps T cell differentiation and proliferation (55).

As suggested by our population coverage analysis, the vaccine candidate's broad immunogenicity across South America and other areas supports its potential for preventing ROCV infections in regions where the virus poses a higher threat. Our proposed ROCV vaccine candidate may contribute to controlling ROCV reemergence and improving access to treatment by potentially ensuring effective epitope presentation in populations with greater exposure risk. In the future, epitope selection for the vaccine candidate could be further optimized based on regional HLA frequencies and other epidemiological data in hopes of maximizing the effectiveness. Importantly, previous research supports the practical application of using *in silico* methods to design epitope-based vaccines. For example, a study by Ribeiro et al. developed a DNA vaccine encoding 18 HIV subtype B CD4+ T cell epitopes, which induced potent CD4+ and CD8+ T cell responses in HLA-expressing mice (56). Additionally, 16

https://doi.org/10.59720/24-279

of the 18 epitopes were recognized by immune cells isolated from HIV-infected patients, demonstrating that *in silico* epitope prediction can help accelerate vaccine development and elicit meaningful immune responses *in vivo*.

Our *in silico* study has identified potential antigenic and non-allergenic epitopes for a multi-epitope vaccine against ROCV. This *in silico* study lays the groundwork for future experimental research toward an effective and safe ROCV vaccine. While these initial findings are promising, they require extensive validation through *in vitro* and *in vivo* experiments to ensure the vaccine's efficacy, safety, and stability. In future, we would like to test the vaccine candidate in mice model to determine the antibody titer, cellular immune response and perform neutralizing antibody titer and viral challenge study.

MATERIALS AND METHODS

Sequence retrieval

The polyprotein and genomic sequence of ROCV were obtained from the NCBI Protein Database, with the accession code YP_009553341.1 (26).

Antigenicity screening

The VaxiJen v2.0 server was used for the antigenicity screening of the viral protein, with a default threshold value of 0.4 (27, 57). This allowed for a view of the entire genome to identify candidate proteins to investigate for the vaccine construct.

T cell and B cell epitope prediction

MHC class I molecules present antigens to CD8+ T cells, while MHC class II molecules present antigens to CD4+ T cells. T cells recognize these epitopes in the context of MHC presentation. The IEDB server, which contains a wide array of key information on antibodies and epitopes, served as a platform to generate the B cell and T cell epitopes that were incorporated into the ROCV vaccine candidate (28, 58).

Physicochemical property prediction

In this step, to assess the antigenicity of the original B-cell and T-cell epitopes, the VaxiJen v2.0 server was utilized, with a threshold of 0.4 (57). The AllerTOP v2.0 server was then

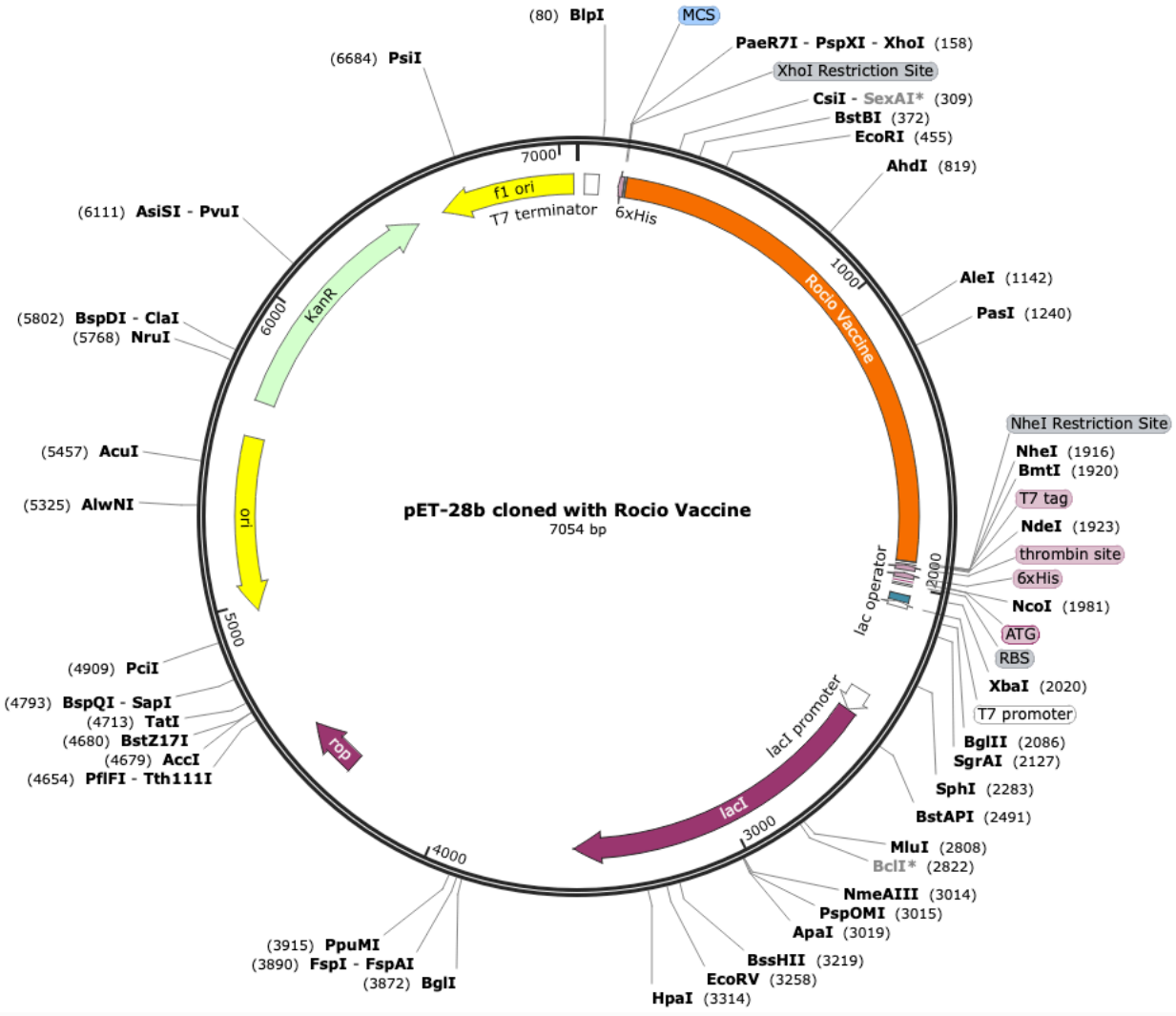

Figure 6: pET-28b vector plasmid cloned with ROCV. The ROCV vaccine DNA was incorporated into pET-28b plasmid using *XhoI* and *NheI* restriction enzyme sites, highlighted in grey. The KanR (kanamycin resistance) gene is highlighted in green, while the orange-colored gene indicates ROCV.

https://doi.org/10.59720/24-279

used to predict the allergenicity of all epitopes, assessing their potential to induce an allergic reaction (59). Additionally, the ToxinPred server supplied information on the toxicity of all epitopes, providing either a positive or negative Support Vector Machine (SVM) score that indicated a toxin or non-toxin, respectively (60). The human homology prediction was performed using the IEDB Epitope Conservancy Analysis server using the BLAST tool provided in the server (61). Expasy ProtParam was used to predict the various physicochemical properties of the candidate, along with the CamSol server to predict the vaccine's intrinsic solubility score (62).

Determination of cytokine-inducing potential

The IFNepitope server was used to calculate the IFN-γ producing ability of the predicted epitopes (63). This server employs an algorithm that determines if an epitope induces cytokine production, comparing it against a dataset of inducing and non-inducing epitopes (64). Additionally, IL-10-inducing characteristics were evaluated using the IL-10Pred server (65, 66).

Population coverage calculation

For the population coverage of our epitopes, we used the IEDB server to examine the favorable epitopes across several HLA alleles in different parts of the world (58, 67). The calculation of population coverage required MHC-restricted alleles to compute, so both the IEDB MHC-I and MHC-II binding prediction servers were used to predict the most promising HLA alleles for each epitope (68, 69).

Epitope display using M13 bacteriophage

We aimed to demonstrate both a phage-based display and a bacterial expression system for vaccine production. Initially, we constructed a model using an M13-based display system with the pIII protein **(Figure 7a–d)**. pIII is a minor coat protein of M13, which is widely used as a fusion partner for different peptides (70). Due to its capability to display large peptides, we used the pIII protein as a fusion partner in our study (71). For epitope display in the M13 bacteriophage, two main approaches are used: a phagemid-based display and a phage-based vector approach. We selected the latter because when the vector has a single copy of the recombinant gene, it results in a polyvalent display where multiple copies of the antigen are presented on the phage surface, enhancing immunogenicity. In contrast, the phagemid-based display, which uses a phagemid vector (a cloning vector that combines characteristics of plasmids and phages), typically results in a monovalent display, where antigen presentation is limited to only a single copy of the antigen, limiting its immunogenicity potential (72). We selected a polyvalent approach to our phage display since the polyvalent display produces and binds more proteins than the monovalent display. Moreover, we incorporated a flexible glycine-rich linker, GGGS, between pIII and the epitopes.

ROCV vaccine construction

For *E. coli* expression, predicted epitopes underwent an extensive screening process, and then were incorporated into the vaccine candidate – for example, only those with an antigenicity score from VaxiJen 2.0 above the threshold of 0.4 (which indicated categorization of "antigen-inducing") and a negative SVM score (corresponding to a non-toxic

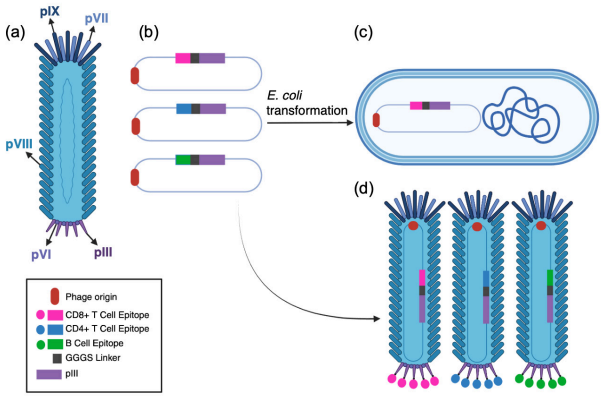

Figure 7: Schematic representation of M13-based epitope display. (a) M13 genome depicting various proteins, including pIII, pVI, pVII, pVIII, and pIX. (b) M13 phage vector containing the phage origin of replication (red) and a GGGS linker (black) connected to three different classes of ROCV peptides with the pIII gene. CD8+ T cell epitopes are shown in pink, CD4+ T cell epitopes in blue, and B cell epitopes in green. (c) Transformation of the M13 phage vector into *E. coli* bacteria. (d) Display of the ROCV antigen using the M13 bacteriophage. Created in BioRender. TASLEM MOUROSI, J. (2026) https://BioRender.com/kmjqlwk

epitope) were selected. Additionally, specifically for the CD4+ T cell epitopes, if an epitope produced a positive IFN score, indicative of an IFN-γ-inducing characteristic, then it passed this additional round of screening only present for the CD4+ T cell epitopes.

We also incorporated different linkers to fuse with the different types of epitopes and integrated the entire sequence into the pET-28b plasmid **(Figure 3a)**. We chose the pET-28b plasmid due to its strong T7 promoter that enables high protein production, and its His-tags present at the N-terminus and C-terminus of the plasmid, which allows for affinity purification (73). At the beginning of vaccine construct, we included the PADRE sequence AKFVAAWTLKAAA, which is a pan-DR-binding epitope known for its capability as a universal synthetic peptide-binding receptor, augmenting CD4+ T cell response through MHC II presentation (74). We used a flexible GGGS linker between the cytotoxic T cell epitopes and a GPGPG linker between the helper T cell epitopes, as commonly employed in fusion proteins to induce immunity (44). Lastly, between the B cell epitopes, we implemented a bi-lysine KK linker, a target sequence engaged in antigenic peptide processing and enhancing antigen presentation, to further increase the overall immunogenicity of our vaccine (75, 76).

Protein structure prediction and molecular docking analysis

To predict the protein's 3-D structure, we utilized Neurosnap AI AlphaFold, which uses the newly developed CASP14 and provides highly accurate results (31). We docked our vaccine candidate with three antigen receptors in protein-protein docking analysis – BCR (PDB ID: 5DRX), a CD4+ T cell receptor (PDB ID: 2NY1), and a CD8+ T cell receptor (PDB ID: 3QZW) through the ClusPro v2.0 server (34). This server utilizes a clustering algorithm that generates thousands of genetic conformations, identifying the most appropriate fits and providing a statistic on the lowest energy level indicative of

https://doi.org/10.59720/24-279

the strongest binding affinity. From the generated models, we selected the one with the lowest energy level, which exhibited a highly populated cluster at the center (77).

Immune simulation

To conduct an immune simulation study, we used the C-ImmSim server, which uses a Position Specific Scoring Matrix (PSSM)-based method to predict immune interactions induced by the vaccine (35). Using the default settings for host HLA selection, including MHC Class I (A01:01), MHC Class I (B07:02), and MHC Class II (DRB1*01:01), we kept all parameters at their default setting except for the time intervals between the three injections set at 1, 84, and 170 time steps—which each represent 8 hours—respectively, attempting to test the immune response over a six-month period. Additionally, the server's total number of simulation steps was set at 1050 (78).

In silico cloning and mRNA secondary structure prediction

For codon optimization, we used the Java Codon Adaptation Tool (JCat) server to generate an optimized codon sequence and to calculate the corresponding codon adaptation index (CAI) and GC-content percentage (36). The ideal CAI value is 1.0, but a score greater than 0.8 is adequate (79). The ideal GC-content percentages span from 30 to 70% (79). During the *in silico* cloning simulation, a high-expression vector pET-28b, which has kanamycin antibiotic resistance, was selected. This protein sequence was reverse-translated and the SnapGene restriction cloning software was utilized to incorporate the vaccine DNA into the plasmid using *XhoI* and *NheI* restriction enzyme sites (80). We used the RNAfold server to generate the mRNA secondary structure of the vaccine construct (37).

Received: July 01, 2024
Accepted: January 05, 2026
Published: August 21, 2026

REFERENCES

1. Tanaka, H., et al. "The Replication of Rocio Virus in Brain Tissue of Suckling Mice. Study by Electron Microscopy." *Archives of Virology*, vol. 78, no. 3, Sep. 1983, pp. 309-314. https://doi.org/10.1007/BF01311327
2. Sagini, João Pedro, et al. "Rocio Virus Encephalitis: *In Silico* Evidence for Drug Repurposing." *Macromolecules*, vol. 2, no. 1, 13 Feb. 2022, pp. 100–112. https://doi.org/10.3390/macromol2010006
3. Saivish, Marielena V., et al. "Detection of Rocio Virus SPH 34675 during Dengue Epidemics, Brazil, 2011–2013." *Emerging Infectious Diseases*, vol. 26, no. 4, Apr. 2020, pp. 797–799. https://doi.org/10.3201/2604.190487
4. De Souza Lopes, Oscar, et al. "Emergence of a New Arbovirus Disease in Brazil." *American Journal of Epidemiology*, vol. 108, no. 5, Nov. 1978, pp. 394–401. https://doi.org/10.1093/oxfordjournals.aje.a112637
5. De Souza Lopes, Oscar, et al. "Avaliação Sorológica de Vacina Contra a Encefalite Humana Causada Pelo Vírus Rocio." *Revista Do Instituto de Medicina Tropical de Sao Paulo*, vol. 22, no. 3, 1980, pp. 108–113.
6. Lorenz, Camila, et al. "Impact of Environmental Factors on Neglected Emerging Arboviral Diseases." *PLOS Neglected Tropical Diseases*, vol. 11, no. 9, 2017, p. e0005959. https://doi.org/10.1371/journal.pntd.0005959
7. Shi, Jiandong, et al. "Epitope-Based Vaccine Target Screening against Highly Pathogenic MERS-COV: An *in Silico* Approach Applied to Emerging Infectious Diseases." *PLOS One*, vol. 10, no. 12, 7 Dec. 2015. https://doi.org/10.1371/journal.pone.0144475
8. Rock, Kenneth L., et al. "Present Yourself! By MHC Class I and MHC Class II Molecules." *Trends in Immunology*, vol. 37, no. 11, Nov. 2016, pp. 724–737. https://doi.org/10.1016/j.it.2016.08.010
9. Sette, Alessandro, and John Fikes. "Epitope-Based Vaccines: An Update on Epitope Identification, Vaccine Design and Delivery." *Current Opinion in Immunology*, vol. 15, no. 4, Aug. 2003, pp. 461–470. https://doi.org/10.1016/s0952-7915(03)00083-9
10. Abd-Aziz, Noraini, and Chit Laa Poh. "Development of Peptide-Based Vaccines for Cancer." *Journal of Oncology*, vol. 2022, 15 Mar. 2022, pp. 1–17. https://doi.org/10.1155/2022/9749363
11. Moin, Abu Tayab, et al. "A Computational Approach to Design a Polyvalent Vaccine against Human Respiratory Syncytial Virus." *Scientific Reports*, vol. 13, no. 1, 15 June 2023. https://doi.org/10.1038/s41598-023-35309-y
12. Antonelli, Ana Clara Barbosa, et al. "*In Silico* Construction of a Multiepitope Zika Virus Vaccine Using Immunoinformatics Tools." *Scientific Reports*, vol. 12, no. 1, 4 Jan. 2022, pp. 53. https://doi.org/10.1038/s41598-021-04208-8
13. Elliott, Suzanne L., et al. "Phase I Trial of a CD8+ T-Cell Peptide Epitope-Based Vaccine for Infectious Mononucleosis." *Journal of Virology*, vol. 82, no. 3, Feb. 2008, pp. 1448–1457. https://doi.org/10.1128/jvi.01409-07
14. Slingluff, Craig L., et al. "A Randomized Phase II Trial of Multiepitope Vaccination with Melanoma Peptides for Cytotoxic T Cells and Helper T Cells for Patients with Metastatic Melanoma (E1602)." *Clinical Cancer Research*, vol. 19, no. 15, 31 July 2013, pp. 4228–4238. https://doi.org/10.1158/1078-0432.ccr-13-0002
15. Patronov, Atanas, and Irini Doytchinova. "T-Cell Epitope Vaccine Design by Immunoinformatics." *Open Biology*, vol. 3, no. 1, Jan. 2013, pp. 120139. https://doi.org/10.1098/rsob.120139
16. Tao, Pan, et al. "A Bacteriophage T4 Nanoparticle-Based Dual Vaccine against Anthrax and Plague." *mBio*, vol. 9, no. 5, Sept. 2018, pp. e01926-18. https://doi.org/10.1128/mbio.01926-18
17. Zhu, Jingen, et al. "A Universal Bacteriophage T4 Nanoparticle Platform to Design Multiplex SARS-CoV-2 Vaccine Candidates by CRISPR Engineering." *Science Advances*, vol. 7, no. 37, 10 Sept. 2021, pp. eabh1547. https://doi.org/10.1126/sciadv.abh1547
18. Hashiguchi, Shuhei, et al. "Immunological Basis of M13 Phage Vaccine: Regulation under Myd88 and TLR9 Signaling." *Biochemical and Biophysical Research Communications*, vol. 402, no. 1, Nov. 2010, pp. 19–22. https://doi.org/10.1016/j.bbrc.2010.09.094
19. Hess, Krystina L., and Christopher M. Jewell. "Phage Display as a Tool for Vaccine and Immunotherapy Development." *Bioengineering & Translational Medicine*, vol. 5, no. 1, 18 Sept. 2019. https://doi.org/10.1002/btm2.10142
20. Ebrahimizadeh, Walead, and Masoumeh Rajabibazl.

"Bacteriophage Vehicles for Phage Display: Biology, Mechanism, and Application." *Current Microbiology*, vol. 69, no. 2, 18 Mar. 2014, pp. 109–120. https://doi.org/10.1007/s00284-014-0557-0
21. Zhu, Jingen, et al. "A Bacteriophage-Based, Highly Efficacious, Needle- and Adjuvant-Free, Mucosal COVID-19 Vaccine." *mBio*, vol. 13, no. 4, 2 Aug. 2022, pp. e01822-22. https://doi.org/10.1128/mbio.01822-22
22. Palma, Marco. "Aspects of Phage-Based Vaccines for Protein and Epitope Immunization." *Vaccines*, vol. 11, no. 2, pp. 436. https://doi.org/10.3390/vaccines11020436
23. Cid, Rosa, and Julio Bolívar. "Platforms for Production of Protein-Based Vaccines: From Classical to Next-Generation Strategies." *Biomolecules*, vol. 11, no. 8, 21 July 2021, pp. 1072. https://doi.org/10.3390/biom11081072
24. Magalhães, Perola O., et al. "Methods of Endotoxin Removal from Biological Preparations: A Review." *Journal of Pharmaceutical Sciences*, vol. 10, 2011, pp. 1–15.
25. Ducker, Charles, et al. "Comparative Analysis of Protein Expression Systems and PTM Landscape in the Study of Transcription Factor ELK-1." *Protein Expression and Purification*, vol. 203, March 2023, p. 106216. https://doi.org/10.1016/j.pep.2023.106216
26. "polyprotein [Rocio virus]." *National Library of Medicine*, *National Center for Biotechnology Information*. https://www.ncbi.nlm.nih.gov/protein/YP_009553341.1
27. "VaxiJen: Prediction of Protective Antigens and Subunit Vaccines." *Edward Jenner Institute*. https://www.ddg-pharmfac.net/vaxijen/VaxiJen/VaxiJen.html. Accessed 12 Aug. 2023.
28. "IEDB: Immune Epitope Database." *IEDB*. https://www.iedb.org/. Accessed 08 Aug. 2023.
29. Carlini, Valentina, et al. "The Multifaceted Nature of IL-10: Regulation, Role in Immunological Homeostasis and Its Relevance to Cancer, COVID-19 and Post-COVID Conditions." *Frontiers in Immunology*, vol. 14, 6 July 2023, pp. 1161067. https://doi.org/10.3389/fimmu.2023.1161067
30. Misra, Namrata, et al. "Population Coverage Analysis of T-Cell Epitopes of *Neisseria Meningitidis* Serogroup B from Iron Acquisition Proteins for Vaccine Design." *Bioinformation*, vol. 6, no. 7, 2011, pp. 255. https://doi.org/10.6026/97320630006255
31. Jumper, John, et al. "Highly Accurate Protein Structure Prediction with AlphaFold." *Nature*, vol. 596, no. 7873, 15 July 2021, pp. 583–589. https://doi.org/10.1038/s41586-021-03819-2
32. Janeway, Charles A., et al. "Antigen Recognition by B-Cell and T-Cell Receptors." *Immunobiology: The Immune System in Health and Disease*, 2001, pp. 103–134.
33. Hoque, Hammadul, et al. "Implementation of *In Silico* Methods to Predict Common Epitopes for Vaccine Development against Chikungunya and Mayaro Viruses." *Heliyon*, vol. 7, no. 3, 2021. https://doi.org/10.1016/j.heliyon.2021.e06396
34. "ClusPro 2.0." *Boston University*. https://cluspro.bu.edu/login.php. Accessed 24 Aug. 2023.
35. "C-ImmSim." https://kraken.iac.rm.cnr.it/C-IMMSIM/. Accessed 28 Aug. 2023.
36. "JCat: A Java Codon Adaptation Tool." *JCat*. http://www.jcat.de/. Accessed 30 Aug. 2023.
37. "RNAfold Web Server." *Institute for Theoretical Chemistry, University of Vienna*. http://rna.tbi.univie.ac.at/cgi-bin/RNAWebSuite/RNAfold.cgi. Accessed 31 Aug. 2023.
38. Wang, Rui, et al. "M13 Phage: A Versatile Building Block for a Highly Specific Analysis Platform." *Analytical and Bioanalytical Chemistry*, vol. 415, no. 18, 3 Mar. 2023, pp. 3927–3944. https://doi.org/10.1007/s00216-023-04606-w
39. Malik, Pratap, et al. "Factors Limiting Display of Foreign Peptides on the Major Coat Protein of Filamentous Bacteriophage Capsids and a Potential Role for Leader Peptidase." *FEBS Letters*, vol. 436, no. 2, 2 Oct. 1998, pp. 263–266. https://doi.org/10.1016/s0014-5793(98)01140-5
40. Del Guercio, Marie-France, et al. "Potent Immunogenic Short Linear Peptide Constructs Composed of B Cell Epitopes and Pan Dr T Helper Epitopes (Padre) for Antibody Responses *in Vivo*." *Vaccine*, vol. 15, no. 4, Mar. 1997, pp. 441–448. https://doi.org/10.1016/s0264-410x(97)00186-2
41. Alexander, Jeff, et al. "Development of High Potency Universal DR-Restricted Helper Epitopes by Modification of High Affinity DR-Blocking Peptides." *Immunity*, vol. 1, no. 9, Dec. 1994, pp. 751–761. https://doi.org/10.1016/s1074-7613(94)80017-0
42. Yang, Yi, et al. "*In Silico* Design of a DNA-Based HIV-1 Multi-Epitope Vaccine for Chinese Populations." *Human Vaccines & Immunotherapeutics*, vol. 11, no. 3, 4 Mar. 2015, pp. 795–805. https://doi.org/10.1080/21645515.2015.1012017
43. Reddy Chichili, Vishnu Priyanka, et al. "Linkers in the Structural Biology of Protein–Protein Interactions." *Protein Science*, vol. 22, no. 2, 8 Jan. 2013, pp. 153–167. https://doi.org/10.1002/pro.2206
44. Livingston, Brian, et al. "A Rational Strategy to Design Multiepitope Immunogens Based on Multiple Th Lymphocyte Epitopes." *The Journal of Immunology*, vol. 168, no. 11, 1 June 2002, pp. 5499–5506. https://doi.org/10.4049/jimmunol.168.11.5499
45. Yano, Akira, et al. "An Ingenious Design for Peptide Vaccines." *Vaccine*, vol. 23, no. 17–18, 18 Mar. 2005, pp. 2322–2326. https://doi.org/10.1016/j.vaccine.2005.01.051
46. Stone, Jennifer D., and David M. Kranz. "Role of T Cell Receptor Affinity in the Efficacy and Specificity of Adoptive T Cell Therapies." *Frontiers in Immunology*, vol. 4, 2013, p. 244. https://doi.org/10.3389/fimmu.2013.00244
47. Tan, M. P., et al. "T Cell Receptor Binding Affinity Governs the Functional Profile of Cancer-Specific CD8+ T Cells." *Clinical & Experimental Immunology*, vol. 180, no. 2, 2015, pp. 255–270. https://doi.org/10.1111/cei.12570
48. Tahir ul Qamar, Muhammad, et al. "Designing Multi-Epitope Vaccine against *Staphylococcus Aureus* by Employing Subtractive Proteomics, Reverse Vaccinology and Immuno-Informatics Approaches." *Computers in Biology and Medicine*, vol. 132, May 2021, pp. 104389. https://doi.org/10.1016/j.compbiomed.2021.104389
49. Gasteiger, Elisabeth, et al. "Protein Identification and Analysis Tools on the Expasy Server." *The Proteomics Protocols Handbook*, 2005, pp. 571–607. https://doi.org/10.1385/1-59259-890-0:571
50. Ikai, Atsushi. "Thermostability and Aliphatic Index of Globular Proteins." *The Journal of Biochemistry*, vol. 88,

no. 6, Oct. 1980, pp. 1895–1898. https://doi.org/10.1093/oxfordjournals.jbchem.a133168
51. Ali, Mudassar, et al. "Exploring Dengue Genome to Construct a Multi-Epitope Based Subunit Vaccine by Utilizing Immunoinformatics Approach to Battle against Dengue Infection." *Scientific Reports*, vol. 7, no. 1, 23 Aug. 2017. https://doi.org/10.1038/s41598-017-09199-w
52. Mahmud, Shafi, et al. "Designing a Multi-Epitope Vaccine Candidate to Combat MERS-COV by Employing an Immunoinformatics Approach." *Scientific Reports*, vol. 11, no. 1, 29 July 2021. https://doi.org/10.1038/s41598-021-92176-1
53. Alberts, Bruce, et al. *B Cells and Antibodies. Molecular Biology of the Cell*, 4th ed., Garland Science, 2002, https://www.ncbi.nlm.nih.gov/books/NBK26878/.
54. Zou, Yong-Rui, et al. *B Cells. Kelley and Firestein's Textbook of Rheumatology*, Elsevier, 2017, pp. 207–230.
55. Vaillant, Angel A. J., and Ahmad Qurie. "Interleukin." *StatPearls [Internet]*, StatPearls Publishing, 2022, https://www.ncbi.nlm.nih.gov/books/NBK507821/.
56. Ribeiro, Susan P., et al. "A Vaccine Encoding Conserved Promiscuous HIV CD4 Epitopes Induces Broad T Cell Responses in Mice Transgenic to Multiple Common HLA Class II Molecules." *PLOS One,* vol. 5, no. 6, 11 June 2010, pp. 11072 https://doi.org/10.1371/journal.pone.0011072
57. Doytchinova, Irini A., and Darren R. Flower. "VaxiJen: A Server for Prediction of Protective Antigens, Tumour Antigens and Subunit Vaccines." *BMC Bioinformatics*, vol. 8, no. 1, 5 Jan. 2007. https://doi.org/10.1186/1471-2105-8-4
58. Vita, Randi, et al. "The Immune Epitope Database (IEDB): 2018 Update." *Nucleic Acids Research*, vol. 47, no. D1, 24 Oct. 2018. https://doi.org/10.1093/nar/gky1006
59. Dimitrov, Ivan, et al. "AllerTOP - a Server for *in Silico* Prediction of Allergens." *BMC Bioinformatics*, vol. 14, no. S6, Apr. 2013. https://doi.org/10.1186/1471-2105-14-s6-s4
60. "ToxinPred." *IIIT-Delhi*. https://webs.iiitd.edu.in/raghava/toxinpred/design.php. Accessed 12 Aug. 2023.
61. Bui, Huynh-Hoa, et al. "Development of an Epitope Conservancy Analysis Tool to Facilitate the Design of Epitope-Based Diagnostics and Vaccines." *BMC Bioinformatics*, vol. 8, no. 1, 26 Sep. 2007, pp. 361. https://doi.org/10.1186/1471-2105-8-361
62. Sormanni, Pietro, et al. "The CamSol Method of Rational Design of Protein Mutants with Enhanced Solubility." *Journal of Molecular Biology*, vol. 427, no. 2, 16 Jan. 2015, pp. 478–490. https://doi.org/10.1016/j.jmb.2014.09.026
63. "IFNepitope." *IIIT-Delhi*. http://crdd.osdd.net/raghava/ifnepitope/. Accessed 15 Aug. 2023.
64. Dhanda, Sandeep Kumar, et al. "Designing of Interferon-Gamma Inducing MHC Class-II Binders." *Biology Direct*, vol. 8, no. 1, Dec. 2013. https://doi.org/10.1186/1745-6150-8-30
65. "IL-10Pred: Prediction of Interleukin-10 Inducing Peptides." *IIIT-Delhi*. http://crdd.osdd.net/raghava/IL-10pred/. Accessed 15 Aug. 2023.
66. Nagpal, Gandharva, et al. "Computer-Aided Designing of Immunosuppressive Peptides Based on IL-10 Inducing Potential." *Scientific Reports*, vol. 7, no. 1, 17 Feb. 2017. https://doi.org/10.1038/srep42851
67. "Population Coverage." *IEDB*. http://tools.iedb.org/population/. Accessed 18 Aug. 2023.
68. "MHC-I Binding Predictions." *IEDB*. http://tools.iedb.org/mhci/. Accessed 18 Aug. 2023.
69. "MHC-II Binding Predictions." *IEDB*. http://tools.iedb.org/mhcii/. Accessed 18 Aug. 2023.
70. Smith, George P. "Filamentous Fusion Phage: Novel Expression Vectors That Display Cloned Antigens on the Virion Surface." *Science*, vol. 228, no. 4705, 14 June 1985, pp. 1315–1317. https://doi.org/10.1126/science.4001944
71. Sidhu, Sachdev S, et al. "High Copy Display of Large Proteins on Phage for Functional Selections." *Journal of Molecular Biology*, vol. 296, no. 2, Feb. 2000, pp. 487–495. https://doi.org/10.1006/jmbi.1999.3465
72. Jaroszewicz, Weronika, et al. "Phage Display and Other Peptide Display Technologies." *FEMS Microbiology Reviews*, vol. 46, no. 2, Mar. 2022, pp. fuab052. https://doi.org/10.1093/femsre/fuab052
73. Studier, F. William, and Barbara A. Moffatt. "Use of Bacteriophage T7 RNA Polymerase to Direct Selective High-Level Expression of Cloned Genes." *Journal of Molecular Biology*, vol. 189, no. 1, 4 July 1986, pp. 113–130. https://doi.org/10.1016/0022-2836(86)90385-2
74. Ghaffari-Nazari, Haniyeh, et al. "Improving Multi-Epitope Long Peptide Vaccine Potency by Using a Strategy That Enhances CD4+ T Help in BALB/c Mice." *PLOS One*, vol. 10, no. 11, 11 Nov. 2015, pp. e0142563. https://doi.org/10.1371/journal.pone.0142563
75. Ayyagari, Vijaya Sai, et al. "Design of a Multi-Epitope-Based Vaccine Targeting M-Protein of SARS-Cov2: An Immunoinformatics Approach." *Journal of Biomolecular Structure and Dynamics*, vol. 40, no. 7, 30 Nov. 2020, pp. 2963–2977. https://doi.org/10.1080/07391102.2020.1850357
76. Li, Xiaoyan, et al. "Design and Evaluation of a Multi-Epitope Peptide of Human Metapneumovirus." *Intervirology*, vol. 58, no. 6, 2015, pp. 403–412. https://doi.org/10.1159/000445059
77. Kozakov, Dima, et al. "The ClusPro Web Server for Protein–Protein Docking." *Nature Protocols*, vol. 12, no. 2, 12 Jan. 2017, pp. 255–278. https://doi.org/10.1038/nprot.2016.169
78. Rapin, Nicolas, et al. "Computational Immunology Meets Bioinformatics: The Use of Prediction Tools for Molecular Binding in the Simulation of the Immune System." *PLOS One*, vol. 5, no. 4, 16 Apr. 2010. https://doi.org/10.1371/journal.pone.0009862
79. Huyan, Ting, et al. "Optimized Expression and Purification of Humbug in Pichia Pastoris and Its Monoclonal Antibody Preparation." *Iranian Journal of Public Health*, vol. 44, no. 12, Dec. 2015, pp. 1632–1642.
80. "SnapGene." *SnapGene*. https://www.snapgene.com/. Accessed 30 Aug. 2023.